Analyzing the effect of traffic scenario on conflict count models for unstructured and layered airspaces

Ólafur Þórðarson
Supervisors: Emmanuel Sunil, Joost Ellerbroek, Jacco Hoekstra

***Abstract*—Decentralized airspace concepts have been proposed to increase the capacity of airspace. Previous research has showed that decentralized airspace concepts show great improvements in capacity, such as the Layers concept, where height rules are implemented, and unstructured airspace, where there are no procedural constraints. One aspect that determines capacity is safety. Measuring the number of instantaneous conflicts can be used as an intrinsic safety metric for new airspace design. Conflict counts can be measured by doing experiments which can be time consuming, or by using mathematical models. However, these models are derived using certain assumptions about the traffic. The ideal traffic settings for the models may not always be realistic in practice. This research attempts to improve the models and validate how accurate the models are with varying traffic scenarios, so that the conflict count models may be used for more realistic traffic scenarios.**

***Index Terms*—Decentralized Airspace, Conflict Count Models, BlueSky**

I. Introduction

Air traffic demand is ever increasing. According to Eurocontrol [1] the number of flights per year is expected to increase by about 2.2% annually for the next 7 years. Between 2014 and 2015 delays in flight increased by 23%, which may indicate that there are issues with airspace capacity. Action is needed to increase the capacity of the airspace, either to improve the current en route system or to implement a completely new system.

A system that has been suggested is decentralized airspace [2]. A *centralized* system is where the traffic flow and separation are maintained by a central controller like Air Traffic Control (ATC), but when an airspace concept is *decentralized*, the separation is maintained by the pilots themselves and routes can be chosen by them as well. Recent studies [3] [4] have proposed Unstructured Airspace (UA) and Layered Airspace concepts, which are types of decentralized airspace concepts. The UA concept is where there are no procedural constraints, which gives the pilots complete flexibility in selecting their routes. The only constraints in the UA concept are physical constraints such as terrain and weather. On the other hand, layered concepts apply altitude constraints, and heading-altitude rules are used to determine the cruising altitude of an aircraft.

To ensure safety, and avoid possible collisions, aircraft have a predefined separation zone which is defined with a horizontal and vertical distance. If two aircraft enter each other's separation zone, it is refereed to as an *intrusion*, when an intrusion is predicted it is referred to as a *conflict*. In a decentralized airspace, pilots make use of Conflict Detection (CD) to detect conflicts, which is a part of an on-board aircraft system called Airborne Separation Assurance System (ASAS).

The number of conflicts that occur in an airspace has been used as a metric for *intrinsic safety* which is the ability of the airspace design to prevent conflicts. The analytical conflict count of an airspace design can be obtained by doing experiments or by using conflict count models. Previous studies have made use of conflict count models [4][3], and the accuracy have been found to be high. However the models are derived using assumptions regarding *traffic scenario* properties [5] [6] [7]. A traffic scenario defines the heading and routes for all aircraft in the airspace. The routes include origin and destination points, cruising altitude and the speed. The assumptions that are made in the derivation of these models are:

- Heading distribution is uniform
- Aircraft speeds are equal
- Altitude distribution is uniform
- Traffic density is uniform for the whole airspace

In practice, a traffic scenario with these exact combination of properties is not likely to occur. The question still remains how discarding the model assumptions will affect the accuracy of the model, i.e., if the models are still applicable when the traffic scenario varies from the ideal conditions, and if the accuracy error can be predicted and compensated. Another consideration is whether any assumption affects the accuracy more than other assumptions.

In this research the models will be tested for traffic scenarios which do not respect the above assumptions. This is done by varying the distributions of aircraft headings, speeds, altitude, spatial organization, and speeds for a number of cases. Five experiments will be performed; one assumption will be disregarded in each experiment while respecting all the other assumptions. The results will be compared with an additional experiment with the ideal model settings as a baseline. Furthermore, a numerical approach is proposed to adjust the predictions of the analytical models. The effectiveness of these numerical adjustments is also investigated using the data collected during the simulation experiments. The adjustments are made form complex integrals, which is why a numerical approximation is used.

This paper is structured as follows. The baseline analytical conflict count models will be discussed in Section II. In Section III, the effect of each assumption is analyzed and a numerical approach is used to suggest model corrections for non-ideal traffic scenarios. The experiments and their setup are explained in Section IV. The results from the experiments are presented in Section V and discussed in Section VI. Finally a conclusion is made in Section VII.

II. Analytical Conflict Count Models

The theoretical approach to compute the instantaneous conflict count is to use so-called Conflict Count Models. They consider the maximum possible combinations of two aircraft in the airspace, which is the maximum number of possible conflicts. However, not all of those conflict do occur, so the number of combinations is scaled down with the conflict probability, see Eq. 1, where N_{total} is the number of instantaneous aircraft in the airspace and p_2 is the probability of conflict between two aircraft [2]. This section only summarises the 3D models, but to see the full derivations see [6] and [7].

$$C_{total} = \binom{N_{total}}{2} p_2 = \frac{N_{total}}{2}(N_{total}-1)\ p_2 \tag{1}$$

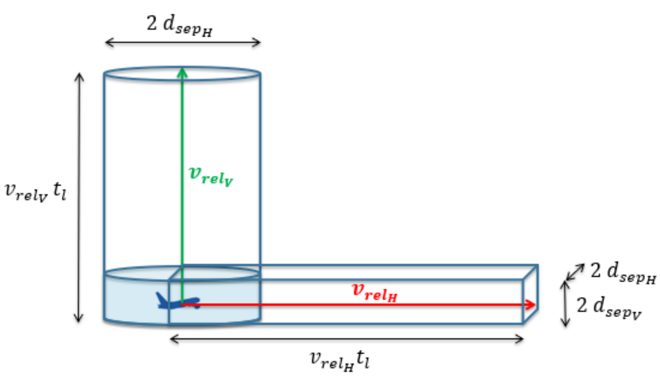

Figure 1. *The volume searched by the CD. [7]*

Conflict probability is the chance of two aircraft trajectories getting too close in the future. The conflict probability is based on the ratio between an area/volume of airspace that an aircraft searches for conflicts during conflict detection (CD) (see Figure 1), and total area/volume of the airspace region . The choice between area and volume depends on the phase of flight, and the specific airspace design under consideration. The models used in this study include climbing and descending aircraft for both UA and Layered airspace. These models are adapted from [6] and [8] in a paper by Sunil et al. [7].

A. Unstructured Airspace

When Unstructured Airspace (UA), there are no procedural constraints regarding the air traffic. The pilots can choose their own direction and altitude. Consequently, the conflict count model for UA does not consider the flight phase of an aircraft.

The model for the UA concept is presented in Eq. 2. The symbols in the equations are described in Table I

Table I
SYMBOLS USED FOR THE MODEL.

Horizontal Separation	d_{sep_h}
Vertical Separation	d_{sep_v}
Expected Horizontal Relative Velocity	$\bar{v}_{rel_h}$
Expected Vertical Relative Velocity	$\bar{v}_{rel_v}$
Look-ahead	t_L
Average Speed	v
Climbing/Descending Angle	$\gamma_{C/D}$
Ratio of Cruising Aircraft	ϵ
Heading Range	α

$$C_{total_{UA,3D}} = \frac{N_{total}}{2}(N_{total}-1)\ p_{2_{UA,3D}} \tag{2a}$$

$$p_{2_{UA,3D}} = \frac{4\ d_{sep_h} d_{sep_v} \bar{v}_{rel_h}\ t_L}{V_{total}} + \frac{\pi\ d_{sep_h}^2 \bar{v}_{rel_v}\ t_L}{V_{total}} \tag{2b}$$

$$\bar{v}_{rel_h} = \frac{4v}{\pi} \tag{2c}$$

$$\bar{v}_{rel_v} = v\sin(\gamma_{C/D})(1-\epsilon^2) \tag{2d}$$

$$\epsilon = \frac{N_{cruise}}{N_{total}} \tag{2e}$$

B. Layered Airspace

In layered airspace concepts, the cruising altitude of an aircraft depends on its heading, and this is defined using heading-altitude rules. These heading-altitude rules specify the heading range, α, which is allowed in each altitude band. Furthermore, the spacing between the altitude bands is at least equal to the vertical separation requirement to prevent conflicts between cruising aircraft in different altitude layers. In these two ways, layered airspaces aim to reduce the probability of conflict when compared to UA. Figure 2 gives a visual description of a layered concept.

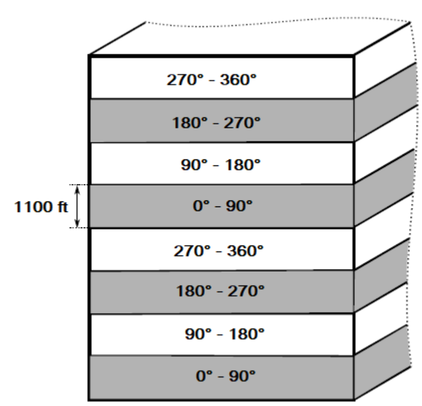

Figure 2. *A visualization of a layered concept, with a heading range of $\alpha = 90°$. Adapted from [3].*

The model for Layered airspace is derived in [6] as a 2D model, but then expanded to 3D model in [7] where climbing and descending aircraft are included. The model for the Layered concept needs to consider the number of aircraft per layer. Because the layered airspace design only applies constraints on cruising aircraft, the conflict count model layered airspaces is composed of three parts; a part that counts the number of conflicts between cruising aircraft, C_{cruise}, a part that considers conflicts between cruising and climbing/descending aircraft,$C_{cruise-C/D}$, and a part for conflicts between climbing/descending aircraft, $C_{C/D}$:

$$C_{SS_{Lay}} = C_{cruise} + C_{cruise-C/D} + C_{C/D} \tag{3}$$

The conflict count model between the cruising aircraft is the same as for the 2D and 3D cases, as there are no climbing or descending aircraft to be considered. In Eq. 4, N_{cruise} is the number of cruising aircraft, L is the number of altitude layers, A_{total} is the total area of the airspace and α is the size of the heading range per altitude band.

$$C_{cruise} = \frac{N_{cruise}}{2}\left(\frac{N_{cruise}}{L} - 1\right)\ p_{2_{cruise}} \tag{4a}$$

$$p_{2_{cruise}} = \frac{2\ d_{sep_h}\bar{v}_{rel_h}\ t_L}{A_{total}} \tag{4b}$$

$$\bar{v}_{rel_h} = \frac{8v}{\alpha}\left(1 - \frac{2}{\alpha}\sin\frac{\alpha}{2}\right) \tag{4c}$$

The $C_{cruise-C/D}$ part of Eq. 3 is the conflict count for conflicts between a cruising aircraft and climbing or descending aircraft. The number of possible combinations of aircraft is a bit different here than for the other case and the conflict probability is based on the volume.

$$C_{cruise-C/D} = N_{cruise}\ N_{C/D}\ p_{2_{cruise-C/D}} \tag{5a}$$

$$p_{2_{cruise-C/D}} = \frac{4\ d_{sep_h}d_{sep_v}\bar{v}_{rel_h}\ t_L}{V_{total}} + \frac{\pi\ d_{sep_h}^2\bar{v}_{rel_v}\ t_L}{V_{total}} \tag{5b}$$

$$\bar{v}_{rel_h} = \frac{4v}{\pi} \tag{5c}$$

$$\bar{v}_{rel_v} = 2v\sin(\gamma_{C/D})(\epsilon - \epsilon^2) \tag{5d}$$

$$\epsilon = \frac{N_{cruse}}{N_{total}} \tag{5e}$$

The final part of the Conflict Count model for layered airspace considers aircraft that are climbing or descending. Here the conflict probability is based on the volume as well, thus it has to include the expected vertical relative velocity, $\bar{v}_{rel_v}$.

$$C_{C/D} = \frac{N_{C/D}}{2}\left(N_{C/D} - 1\right)\ p_{2_{C/D}} \tag{6a}$$

$$p_{2_{C/D}} = \frac{4\ d_{sep_h}d_{sep_v}\bar{v}_{rel_h}\ t_L}{V_{total}} + \frac{\pi\ d_{sep_h}^2\bar{v}_{rel_v}\ t_L}{V_{total}} \tag{6b}$$

$$\bar{v}_{rel_h} = \frac{4v}{\pi} \tag{6c}$$

$$\bar{v}_{rel_v} = v\sin(\gamma_{C/D})(1 - \epsilon)^2 \tag{6d}$$

Now Eqs. 4, 5 and 6 are substituted in Eq. 3, to get the final Conflict Count model for the Layered Airspace concepts.

III. Adjusted Conflict Count Models

As mentioned before, several assumptions concerning the heading, speed, altitude and spatial distribution of traffic are made during the derivation of the analytical conflict count models. These assumptions are expected to lead to inaccurate conflict count predictions, if they are not respected. It is hypothesized that the errors can be predicted and compensated for by making adjustments to the model. By analysing the assumptions and where they affect the equations, the adjustments can be derived and included in the model to make them more adaptable to the traffic scenario.

The changes to the model are to be validated by fitting the experiment results with the adjusted models to investigate the accuracies. As the experiments are designed so the traffic follows a specific heading, speed, altitude and spatial distributions. The same distributions that are used in the experiments are used in the derivations of the adjustments.

A. Heading Distribution Adjustment

When deriving the expected horizontal relative velocity ($\bar{v}_{rel_h}$), in Section II it is assumed that the heading distribution is uniform. There are two parts in finding $\bar{v}_{rel_h}$, the probability density function for the absolute heading difference ($P(|\Delta hdg|)$), and the relative velocity ($v_{rel_h}(|\Delta hdg|)$), see equation 7. $|\Delta hdg|$ is the distribution of the absolute heading difference, in Figure 3 the probability density function of the absolute heading difference for uniform heading distribution can be seen.

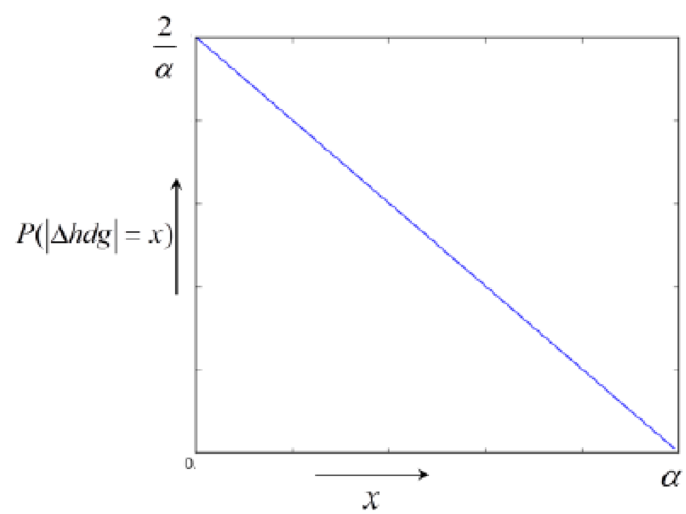

Figure 3. *The distribution of the absolute heading difference for uniformly distributed heading.*

$$\bar{v}_{rel_h} = \int_0^{\alpha} P(x = |\Delta hdg|)\ v_{rel_h}(x = |\Delta hdg|)dx \tag{7a}$$

$$v_{rel_h}(x) = 2v\sin\left(\frac{x}{2}\right) \tag{7b}$$

$$P(x) = \frac{2}{\alpha}\left(1 - \frac{x}{\alpha}\right) \tag{7c}$$

When the heading distribution is uniform, the expected horizontal relative velocity is as described in Eqs. 2c, 4c, 5c, 6c and Figure 3. But when using different heading distributions these equations are not valid. For these cases, new probability density functions need to be defined instead of Eq. 7c.

Three different heading distributions were chosen to be tested in this research. Normal distribution was chosen to simulate traffic that is mostly heading relatively in the same direction, ranged-uniform distribution was chosen to be similar to the normal distribution, but to be more spread out. These two distributions can be an example of traffic moving towards oceanic airspace in the morning for example where there is no head-on traffic. A bimodal distribution was chosen to simulate head-on traffic, for example like when aircraft are in a narrow sector and meet head on traffic. These distributions are shown in Figure 4. For the numerical adjustment for these distributions, the corresponding probability density functions of absolute heading difference need to be used:

$$P(x)_{normal} = \frac{\sqrt{2}}{\sigma\sqrt{\pi}} e^{-\frac{x^2}{2\sigma^2}} \tag{8}$$

$$P(x)_{bimodal} = \frac{1}{2\sqrt{2\pi\sigma^2}} e^{\frac{(x-\pi)^2}{2\sigma^2}} + \frac{1}{\sqrt{2\pi\sigma^2}} e^{-\frac{x^2}{2\sigma^2}} \tag{9}$$

$$P(x)_{ranged-uniform} = \frac{4}{\alpha^2}(\alpha - 2x) \tag{10}$$

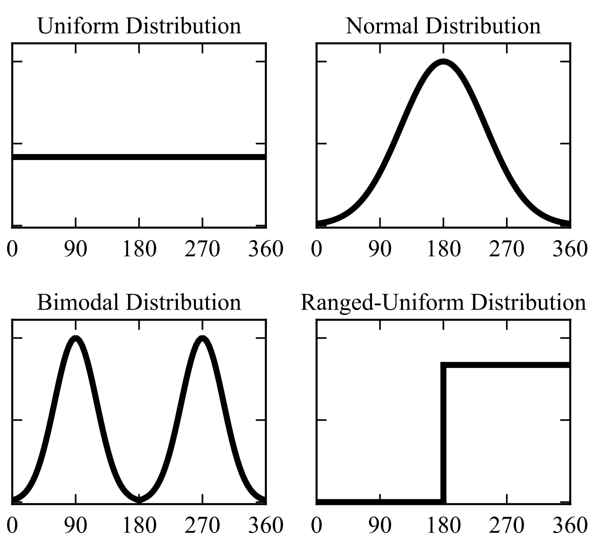

Figure 4. *The probability density functions for the four heading distributions used in the heading experiments.*

Inserting these equations into Eq. 7 instead of Eq. 7c, results in the expected horizontal relative velocity for different heading distribution. Using numerical evaluation, the values for $\bar{v}_{rel_h}$ were obtained and are listed in Table II. The evaluations are only done for airspace concepts that have an $\alpha = 360°$ heading range. For layered concepts with smaller heading range, the altitude distribution would not remain uniform if the heading is not uniform as well.Since the goal of the simulation experiments is to only vary one traffic scenario assumption at a time, only UA and a layered concept with $\alpha = 360^o$ are, therefore, considered for testing the heading distribution adjustment.

Table II
NUMERICALLY COMPUTED VALUES FOR $\bar{v}_{rel_h}$ FOR DIFFERENT HEADING DISTRIBUTION.

Distribution	$\bar{v}_{rel_h}$	Accuacy
Uniform	509 kts	100%
Bimodal	485 kts	95.3%
Normal	395 kts	77.6%
Ranged-Uniform	370 kts	72.7%

The accuracies in Table II are the predicted accuracies and are derived from the error from the $\bar{v}_{rel_h}$ of the uniform distribution. These accuracies are expected to mirror the accuracy of the conflict count model when assuming uniform heading distribution regardless of the actual distribution of aircraft headings. By using the correct $\bar{v}_{rel_h}$ value for the right heading distributions it should be possible to improve the accuracy of the model so it can be valid.

B. Speed Distribution Adjustment

The other part of the derivation of the expected horizontal relative velocity ($\bar{v}_{rel_h}$) is that the speed is assumed to be equal for all aircraft. However, for real life operations, the speeds of aircraft can vary, because of different aircraft types and airline procedures. The relative velocity equation (v_{rel}) in Eq. 7b, is derived from Fig. 5. When the aircraft all have the same speed this equation can be used, but when this is not the case the probability density function of the speed needs to be taken into account. Instead of using Eq. 7b, Eq. 11b is used when aircraft speeds are not equal:

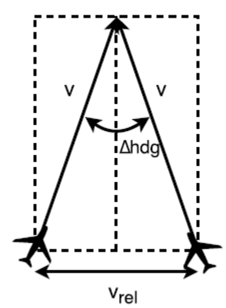

Figure 5. *Representation of relative velocity.[3]*

$$\bar{v}_{rel_h} = \int_{v_1}\int_{v_2}\int_0^{\alpha} v_{rel}(x, v_1, v_2) P(v_1) P(v_2) P(x) dx dv_2 dv_1 \tag{11a}$$

$$v_{rel}(x, v_1, v_2) = (v_1^2 + v_2^2 - 2v_1 v_2 \cos(x))^{\frac{1}{2}} \tag{11b}$$

Here v_1 and v_2 is the speeds for two arbitrary aircraft, x is a stand-in for the absolute heading difference ($|\Delta hdg|$) and where of course the P stands for the corresponding probability density function of speed and heading difference. Numerical evaluation of Eq. 11 can be seen in Table III for different speed distributions. The table shows the speed values for different types of layered concepts. L360 is when the heading range per layer is $\alpha = 360°$. In the L180 concept the layers have heading ranges per layer of $\alpha = 180°$ and L90 with $\alpha = 90°$. The values do not vary significantly from the baseline conditions (all aircraft have equal speed). So it is not expected that the speed has any affect on the accuracy, but should be able to be adjusted by using the right $\bar{v}_{rel_h}$, if it causes inaccuracies.

The three distributions that were tested were uniform-, normal-, and bimodal distributions. Normal distribution to be closer to the baseline scenario where all the aircraft have the same speed, bimodal distribution to have two dominant speeds and uniform distribution is more spread over different speed settings. The probability density functions of the speed distributions can be seen in Figure 6.

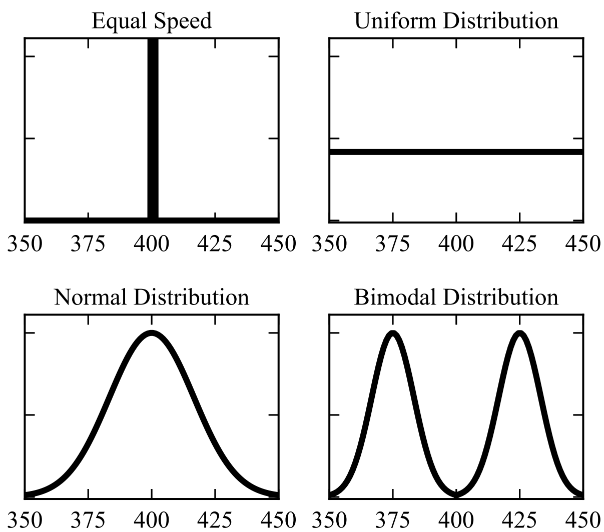

Figure 6. *The probability density functions for the four speed distributions used in the speed experiments.*

Table III
NUMERICALLY COMPUTED VALUES FOR $\bar{v}_{rel_h}$ FOR DIFFERENT SPEED DISTRIBUTION TYPES AND THE RELEVANT ACCURACIES.

Speed Distribution	UA/L360 [kts]	L180 [kts]	L90 [kts]
Equal	509 (100%)	370 (100%)	203 (100%)
Normal	507 (99.61%)	370 (100%)	205 (99.02%)
Bimodal	509 (100%)	373 (99.20%)	208(97.60%)
Uniform	512 (99.41%)	374 (98.93%)	210 (96.67%)

C. Altitude Distribution Adjustment

The model assumption for the altitude has two parts to it. First being the vertical density which affects the UA concept and the other being the number of combination of aircraft for the Layered concepts.

1) Unstructured Airspace: For UA, Eq. 2b shows that conflict probability is computed as the summation of two ratios; 1) the ratio between the volume searched for conflicts in the horizontal direction and the total volume, and 2) the ratio between the volume searched for conflicts in the vertical direction and the total volume. The first of these two ratios assumes a uniform distribution of aircraft cruising altitudes. However, if aircraft are not spread uniformly in the vertical direction, then it is logical that aircraft at busy altitudes experience more conflicts than aircraft in less dense altitudes. The effect of aircraft altitude on conflict probability, p_v, can be calculated as [8]:

$$p_v = \int_{alt_{min}}^{alt_{max}} P(h) \int_{h-d_{sep_v}}^{h+d_{sep_v}} P(z)dz\ dh \tag{12}$$

Here P is the probability density function for the altitude distribution, h is the altitude variable while z is the altitude variable for the other aircraft. When assuming uniform distribution, Eq. 12 becomes:

$$p_{v_{uniform}} = \frac{1}{H} \tag{13}$$

Eq. 13 was implicitly used in the derivation of the 3D conflict probability model given by Eq. 2b:

$$\begin{aligned} p_{2_{UA,3D}} =& \frac{4\ d_{sep_h} d_{sep_v} \bar{v}_{rel_h}\ t_L}{A_{total}} \underbrace{\frac{1}{H}}_{p_{v_{uniform}}} \\ &+ \frac{\pi\ d_{sep_h}^2 \bar{v}_{rel_v}\ t_L}{A_{total}} \underbrace{\frac{1}{H}}_{p_{v_{uniform}}} \end{aligned} \tag{14}$$

Eq. 14 is equivalent to Eq. 2b. But when using an altitude distribution that is not uniform, the probability density function needs to be included in the model, like presented in Eq. 12. Now the conflict count model for unstructured airspace takes on the form as described in Eqs. 15:

$$C_{total_{UA,3D}} = \frac{N_{total}}{2} \left(N_{total} - 1\right)\ p_{2_{UA}} \tag{15a}$$

$$p_{2_{UA}} = \frac{4\ d_{sep_h} d_{sep_v} \bar{v}_{rel_h}\ t_L}{A_{total}} p_v + \frac{\pi\ d_{sep_h}^2 \bar{v}_{rel_v}\ t_L}{A_{total}} p_v \tag{15b}$$

$$p_v = \int_{alt_{min}}^{alt_{max}} P(h) \int_{h-d_{sep_v}}^{h+d_{sep_v}} P(z)dz\ dh \tag{15c}$$

$$\bar{v}_{rel_h} = \frac{8v}{\alpha}\left(1 - \frac{2}{\alpha}\sin\frac{\alpha}{2}\right) \tag{15d}$$

$$\bar{v}_{rel_v} = v\sin(\gamma_{C/D})(1-\epsilon^2) \tag{15e}$$

$$\epsilon = \frac{N_{cruise}}{N_{total}} \tag{15f}$$

When p_v was evaluated numerically for normal, bimodal and ranged uniform altitude distribution (see Figure 7), the corresponding values can be used to adjust the conflict count model, see Table IV where the p_v values and the predicted accuracies are presented. Once again, the 'accuracy' column in this table lists the accuracy of the analytical conflict count model that assumes uniform altitude distribution, regardless of the actual distributions.

Three altitude distributions were tested, normal-, bimodal-, and ranged-uniform. A normal distribution is used to investigate the effect of the case when the traffic is concentrated around one altitude, the bimodal instead to describe concentration of the traffic around two altitudes spreading it more around. Often pilots prefer the upper airspace, that is why a ranged-uniform was chosen where the aircraft are uniformly distributed at higher altitudes. In Figure 7 the probability density functions for the altitude distributions are shown.

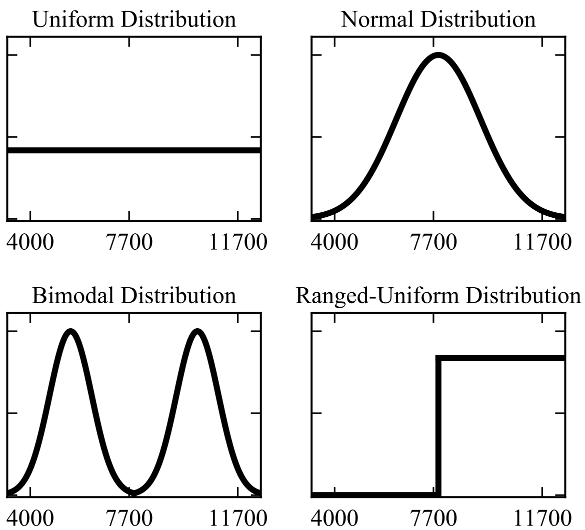

Figure 7. *The probability density functions for the four altitude distributions used in the altitude experiments.*

Table IV
NUMERICALLY COMPUTED VALUES FOR p_v.

Altitude Distribution	p_v	Accuracy
Uniform	0.171	100%
Normal	0.289	59.17%
Bimodal	0.289	59.17%
Ranged Uniform	0.342	50.00%

2) Layers: In the derivation of the Layers concept the number of combinations of aircraft is calculated differently for cruising aircraft, see Eq. 16. Here every layer needs to be considered individually and summed up to get the correct conflict count, see Eqs. 16a and 16b. If the aircraft are evenly spread over the layers (uniform altitude distribution), a simplification to the equation can be made, see Eq. 16c.

$$C_{layer_i} = \frac{N_{layer_i}}{2} (N_{layer_i} - 1)\ p_2 \tag{16a}$$

$$C_{Layers} = \sum_{1}^{L} \frac{N_{layer_i}}{2} (N_{layer_i} - 1)\ p_2 \tag{16b}$$

$$C_{Layers} = \frac{N_{Layers}}{2} (\frac{N_{Layers}}{L} - 1)\ p_2 \tag{16c}$$

When the conflict count models for a layered concepts is applied to a traffic scenario that has a non-uniform altitude distribution, the model is expected to have a low accuracy. If Eq. 16b is used instead of Eq. 16c to calculate the number of combinations of aircraft, then different altitude distributions can be considered. In such cases, the number of aircraft in each layer (N_{layer_i}) should be used. N_{layer_i} is found by creating a set of altitude samples for the various distributions being used, then counting the number of samples within each layer. Using this approach, the number of combinations of two aircraft were calculated for all altitude distributions and all values of N_{total} considered in this work, see Table V.

Table V
NUMBER OF COMBINATIONS OF TWO AIRCRAFT FOR DIFFERENT CRUISING ALTITUDE DISTRIBUTIONS FOR LAYERED AIRSPACES.

N_{total}	Uniform	Normal	Bimodal	Ranged Uniform
80	114	227 (50.22%)	207 (55.07%)	220 (51.82%)
302	1957	3734 (52.41%)	2418 (57.26%)	3960 (49.42%)
589	7655	14507 (52.77%)	13304 (57.54%)	15312 (49.99%)
1146	29069	54907 (52.94%)	50049 (58.08%)	58140 (50.00%)
1600	57000	107128 (53.21%)	98329 (57.97%)	113764 (50.10%)
Average Accuracy	100%	51.32%	57.38%	50.27%

D. Spatial Distribution Adjustment

The analytical model is assumed to have uniform spatial distribution, meaning that the density is the same throughout the airspace it is applied to. The conflict probability is described as the ratio between the volume searched by the conflict detection and the total volume of the airspace. If the traffic density is higher in one place, it stands to reason that the conflict probability is higher within the smaller area, which is referred to as hotspot in this paper.

If the model is applied to specifically the part of the airspace where the hotspot is, and then to the rest of the airspace, the model should give a more accurate conflict count. Figure 8 shows two examples of the two areas used to adjust the model to make it more accurate, with different hotspots, the larger being 55 nm and 40 nm. In Figure 8 there is also an example of the baseline scenario traffic density. Where the areas are marked by the black circles. The inner circle shows the hotspot and the outer circle shows the normal experiment area.

When splitting up the airspace the conflict have to be counted separately for each area. Because the model does not take into account conflicts between the two areas, they must be included as well. Eq. 17 shows the structure of the adjusted model. Where N_{Area_1} is the number of aircraft in the hotspot and N_{Area_2} is the number of aircraft in the rest of the airspace. The conflict probability differs for conflicts within the hotspot($p_{2,Area_1}$), outside the hotspot($p_{2,Area_1}$) and conflicts between aircraft inside and outside the hotspot($p_{2,Area_{1,2}}$).

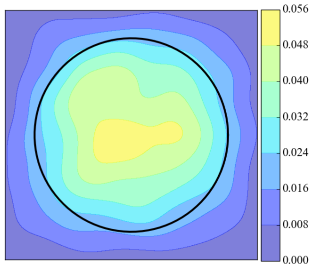

(a) *Baseline*

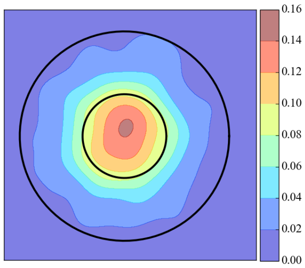

(b) *Hotspot 1, radius 55 nm*

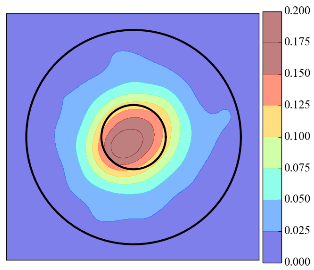

(c) *Hotspot 2, radius 40 nm*

Figure 8. *Traffic density heat maps of the experiment area and the hotspot areas.*

$$C_{total} = C_{Area_1} + C_{Area_2} + C_{Area_{1,2}} \tag{17a}$$

$$C_{Area_1} = \frac{N_{Area_1}}{2}(N_{Area_1} - 1)p_{2,Area_1} \tag{17b}$$

$$C_{Area_2} = \frac{N_{Area_2}}{2}(N_{Area_2} - 1)p_{2,Area_2} \tag{17c}$$

$$C_{Area_{1,2}} = N_{Area_1} N_{Area_2} p_{2,Area_{1,2}} \tag{17d}$$

This adjustments does not include numerical values as the adjustments for the other assumptions are based on. Here the analytical model, described in Section II, is used but applied to hotspot specifically, then to the rest of the airspace.

IV. Experiment Setup

Five fast-time simulation experiments are conducted to determine the accuracy of the conflict rate model. This chapter describes the design of these experiments. Four of the experiments are performed for different heading distributions, spatial distribution, altitude distributions and speed distributions, because these correspond to the four main scenario assumptions made during the derivation of the analytical models. An additional experiment is performed where all the model assumptions are respected. This experiment will be used as a baseline for comparison.

A. Simulation Development

1) Simulation Platform: For the simulations, the open-source ATM simulation platform BlueSky, is used. It is developed in the Python programming language at Delft University of Technology. More information on BlueSky is in [9].

2) Conflict Detection: The CD method used is called state-based conflict detection, where an aircraft's future position is predicted as a linear extrapolation of its position vector assuming constant speeds over a predefined look-ahead time. The conflict is detected when an aircraft's trajectory will violate another aircraft's protected zone as defined by minimum separation. The look-ahead time for CD was five minutes. The separation requirements for CD were 5 NM horizontally, and 1000 ft vertically.

3) Airspace Concepts and Concept Implementation: Four airspace concepts are tested, an unstructured airspace concept with no procedural restrictions and three types of Layered concepts, the concepts are summarized in Table VI. Each Layered concept has a defined heading range per each layer. Sometimes the concepts have more then one layer with the same heading range, this is called layer sets. Table VII shows the separation criteria, the height of each layer, and the lower and higher limit of the airspace.

Table VI
Airspace Concepts

Symbol	Name	Heading Range Per Layer, α	Number of Layer Sets, κ
UA	Unstructured Airspace	-	-
L360	Layers 360	360°	8
L180	Layers 180	180°	4
L90	Layers 90	90°	2

Table VII
Airspace Parameters

Horizontal Separation	Vertical Separation	Layer Height	Altitude Lower Limit	Altitude Upper Limit
5 nm	1000 ft	1100 ft	4000 ft	11700 ft

To implement the concepts, scenarios are modified such that they fit the concept's constraints. The horizontal routes for both UA and Layers concepts are made in the same way. For the unstructured concept, the cruising altitude for the flight is proportional to the flight distance, see Eq. 18a. For the Layers concept the heading as well as the distance determines the altitude, see Eq. 18b. [7]

$$h_{ua} = h_{min} + \frac{h_{max} - h_{min}}{d_{max} - d_{min}}(d - d_{min}) \tag{18a}$$

$$h_{lay} = h_{min} + \tau\left(\left\lfloor \frac{h_{max} - h_{min}}{d_{max} - d_{min}}\kappa \right\rfloor \frac{360°}{\alpha} + \left\lfloor \frac{\psi}{\alpha} \right\rfloor\right) \tag{18b}$$

The above equations describe how the altitude is selected with respect to the distance and heading. Here h is the altitude, d is the distance, ψ is the aircraft's heading, α is the heading range per layer and κ is the number of layer sets. The "$\lfloor ... \rfloor$" is the floor operator.

B. Traffic Scenarios

1) Testing Region and Flight Profiles: The simulation region is 400×400 nm. Origins are chosen based on the spatial distribution type, in most cases uniformly distributed across the whole region. Then the destination point will be chosen according to the heading and distance. The origin

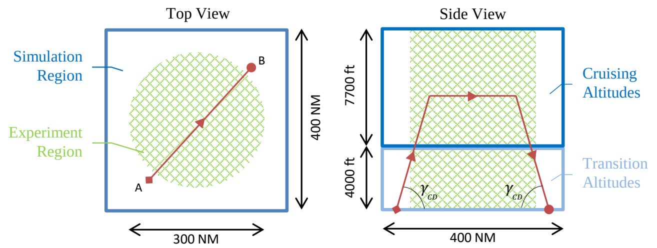

Figure 9. *Top and side view of the simulation environment, an example trajectory is shown. Taken from [7]*

and destination points can be located at any point within the simulation area.

Because the routes need to be within the simulation region, the traffic will be less dense near the edges of the simulation area, and the density will be zero on the edges. The results of the simulation will only be relevant in a specific zone within the simulation region. This is the region where the results will be analyzed in, a circle with a diameter of 300 nautical miles. Figure 9 shows a top and side view of the simulation region. It shows an example of a horizontal and a vertical route.

Aircraft will spawn at the lower boundary of the transition altitudes, see Figure 9, and climb up to their cruising altitude. All aircraft cruise distance. The aircraft will then descent to the destination point. All aircraft have the same climb and descent angle.

2) Scenario Generator: The scenario generator will choose semi-random values for heading, spawning points, distance and speed (only for speed experiments) relevant to the distribution type that is being tested. Using these, it will then compute the correct altitude and which layer is used for the Layers concepts, and choose an appropriate destination point within the simulation area that depends on the heading and distance. Figure 10 shows a flow chart of how the scenario generator works.

For a scenario generation which needs to have a specific spatial distribution the origin points and destination points needs to be specified within a certain area. This is so that the traffic will cross the middle of the area to create a hotspot. For example when creating a density hotspot in the center, the origin points need to be within a specific area determined within two circles, close to the edge of the simulation area. The destination points need to be within another area determined by two circles, close to the center. The sizes of the areas need to be specifically designed with respect to the minimum and maximum distance flown. Figure 11 show examples of origin and destination points plus one trajectory as an example. Because there is a minimum travel distance for aircraft in the simulations, the trajectory is forced though the center of the simulation area. This is caused by the areas which the origin and destination points are in and thus creates a density hotspot.

C. Independent variables

The independent variables of the five experiments performed are given below.

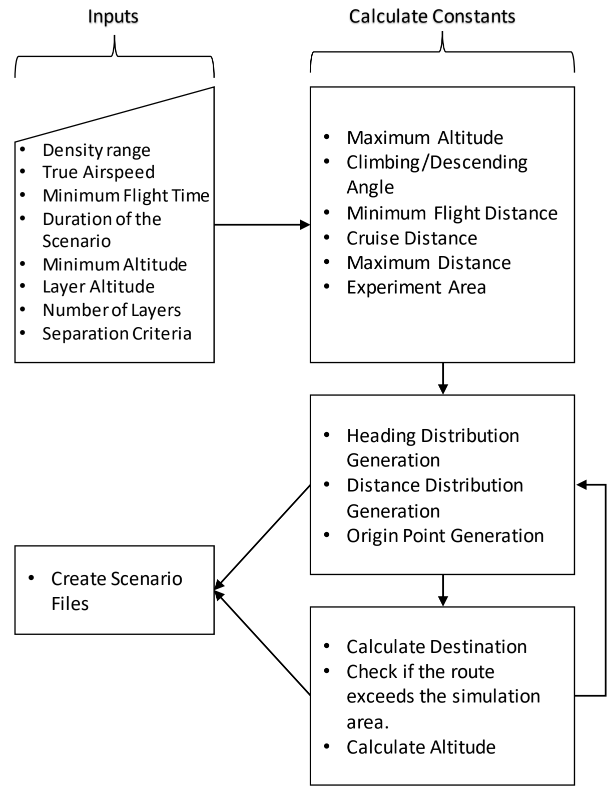

Figure 10. *A flow chart of the scenario generation.*

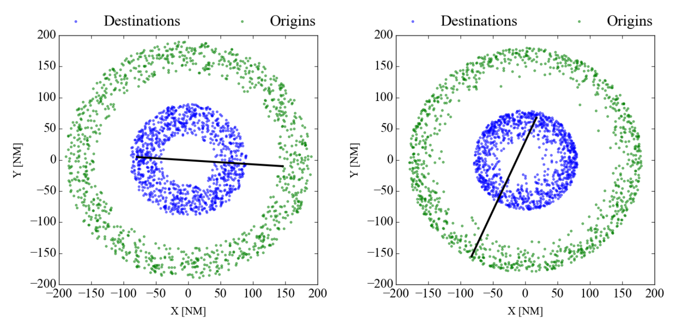

(a) *Hotspot 1* (b) *Hotspot 2*

Figure 11. *The origin (green) and destination (blue) points, with one example trajectory. To the left is the larger hotspot and to the right is the smaller hotspot.*

1) Baseline Experiment:

- Airspace concept: Unstructured Airspace, Layers 360, Layers 180, Layers 90.
- Traffic demand densities: 5 different densities, see Table VIII.

Total number of simulations to run:

- 4 concepts $\times$ 5 densities $\times$ 5 repetitions = 100 simulations.

2) Heading Experiment: The heading experiment is to strictly check the effects of heading distributions other than uniform. It is not realistic that all aircraft have a uniformly distributed heading. The independent variables for the heading experiments are:

Table VIII
TRAFFIC DEMAND SCENARIOS (VALUES FOR SIMULATION REGION)

Density [AC/10000 nm^2]	Number of instantaneous AC
5	80
18	302
36	589
71	1146
100	1600

- Heading distribution, 3 distributions will be tested. Normal distribution, bimodal distribution and ranged normal distribution. See Figure 4.
- Airspace concept: Unstructured Airspace, Layers 360, Layers.
- Traffic demand densities: 5 different densities, see Table VIII.

Total number of simulations to run:

- 3 heading distributions $\times$ 2 concepts $\times$ 5 densities $\times$ 5 repetitions = 150 simulations.

3) Speed Experiment: In the baseline scenario the airspeed is constant, but in this experiment it will vary between aircraft.

- Speed distribution: 3 distributions will be tested, normal distribution, bimodal distribution and uniform distribution. See Figure 6.
- Airspace concept: Unstructured Airspace, Layers 360, Layers 180, Layers 90.
- Traffic demand densities: 5 different densities, see Table VIII

Total number of simulations to run:

- 3 speed distributions $\times$ 4 concepts $\times$ 5 densities $\times$ 5 repetitions = 300 simulations.

4) Altitude Variation Experiment: The altitude is modified by modifying the distance. The altitude distribution is more complicated than the other experiments, as for the Layers 180 and Layers 90 need to have the heading synchronized with the distance. The heading will only remain uniform for the unstructured airspace and Layers 360.

- Altitude distribution: 3 distributions will be tested, normal distribution, bimodal distribution and ranged-uniform. See Figure 7
- Airspace concept: Unstructured Airspace, Layers 360.
- Traffic demand densities: 5 different densities ranging, see Table VIII.

Total number of simulations to run:

- 3 altitude distributions $\times$ 2 concepts $\times$ 5 densities $\times$ 5 repetitions = 150 simulations.

5) Spatial Experiment: This experiment's purpose is to see how the spatial distribution affects the accuracy of the conflict rate model. The spatial distribution is the distribution of aircraft's position within the airspace.

- Spatial distribution: 2 distribution will tested, where there are density hotspot in the middle of the airspace, of different sizes.
- Airspace concept: Unstructured Airspace, Layers 360, Layers 180, Layers 90.
- Traffic demand densities: 5 different densities, see Table VIII.

Total number of simulations to run:

- 2 spatial distribution $\times$ 4 concepts $\times$ 5 densities $\times$ 5 repetitions = 200 simulations.

D. Dependent Variables

The goal is to compare the conflict count computed using the model with the conflict count logged during the simulations, so the two variables that are measured are the instantaneous number of conflict, and the instantaneous number of aircraft. The variables are logged in BlueSky while the simulation is running. To measure the accuracy, an additional parameter is introduced to the models, called the accuracy parameter (k value). See the basic model in Eq. 19.

$$C_{total_{UA}} = \frac{N_{total}}{2}(N_{total} - 1)\ p_2\ k \tag{19}$$

For the Layered concepts the fitting parameter is divided in 3 parts, k_{cruise} for two cruising aircraft conflicting, $k_{cruise-CD}$ for conflicts between cruising and climbing/descending aircraft and k_{CD} for conflicts between climbing/descending aircraft.

$$C_{total_{Lay}} = C_{cruise}k_{cruise} + C_{cruise-CD}k_{cruise-CD} + C_{CD}k_{CD} \tag{20}$$

Eqs. 19 and 20 are fitted to the simulation data using the least squares method where k is used as a fitting parameter. When the k is closer to 1, that means that the model is more accurate. If the parameter is less than 1, we can tell that the model is overestimating because the fitting parameter is less then 1 to scale it down. Also when k is larger than 1 we can tell that the model is underestimating and the fitting parameter is scaling up.

V. RESULTS

In this section the results for the four main experiments will be presented. The result from the baseline experiment is included for comparison with the results from the other experiments.

A. Heading Experiment

1) Effect of heading distribution on conflict count: Figures 12 and 13 show that the number of conflicts is highest when aircraft headings were uniformly distributed. The normal distribution and ranged uniform distribution, are similar but the bimodal distribution is closer to the uniform distribution. The expected horizontal relative velocity, in Table II, is very close for uniform distribution and bimodal distribution, and again close for normal-, and ranged-uniform distribution, and thus the results from the simulations were as expected.

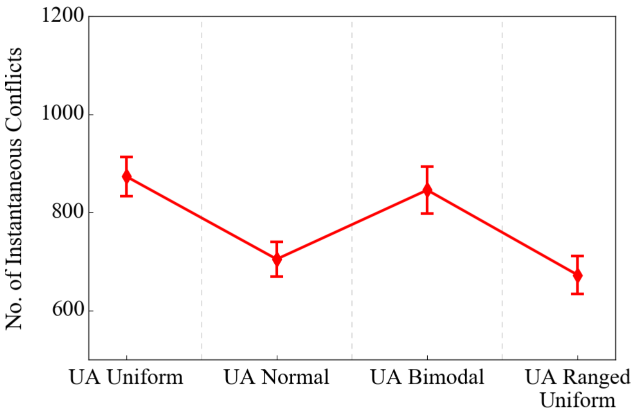

Figure 12. *Heading Experiment - The total number of instantaneous conflicts for the largest density being tested for Unstructured Airspace.*

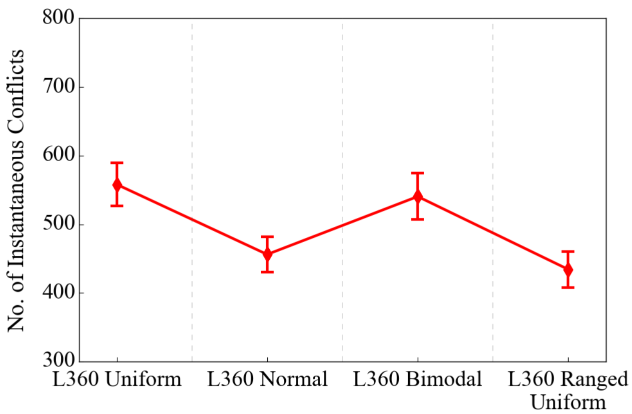

Figure 13. *Heading Experiment - The total number of instantaneous conflicts for the largest density being tested for the Layers 360 concept.*

2) Effect of heading distribution on model accuracy: The results from the experiments were fitted with both the analytical models and the adjusted models. The model accuracies of the analytical model are in Table IX, where the baseline scenario is the uniformly distributed heading. The accuracies of the normal-, and ranged-uniform distribution decrease, but the bimodal distribution does not cause much inaccuracies. The ranged-uniform has the worst accuracy, most likely because the relative horizontal velocity is the furthest away from the value that the baseline scenario has. Table II shows how the accuracies were predicted based on the difference in expected horizontal relative velocity. The accuracy results, for the analytical model, turned out as expected.

The accuracies using the numerically computed values to adjust the model are presented in Table X. The accuracy of the models generally increase. This is the case for both UA and Layered airspaces. The only case where there is a slight dip in accuracy is for the bimodal distribution. The reason for this decrease in accuracy is most likely that simulations are of course a stochastic process. In general the numerical adjustments worked really well when applied to the model.

Table IX
HEADING: BASELINE k VALUES AND ACCURACY.

		Baseline Uniform	Normal	Bimodal	Ranged Uniform
UA	k	1.024 (97.6%)	0.812 (76.8%)	1.004 (99.5%)	0.768 (69.9%)
L360	k_{cruise}	1.004 (99.5%)	0.779 (71.7%)	0.997 (99.7%)	0.735 (64.0%)
	$k_{cruise-CD}$	0.900 (88.9%)	0.761 (68.6%)	0.870 (85.0%)	0.725 (62.1%)
	k_{CD}	0.812 (76.9%)	0.676 (52.2%)	0.739 (64.7%)	0.628 (40.8%)

Table X
HEADING: ADJUSTED k VALUES AND ACCURACY.

		Baseline Uniform	Normal	Bimodal	Ranged Uniform
UA	k	1.024 (97.6%)	0.982 (98.1%)	1.041 (96.0%)	0.974 (97.3%)
L360	k_{cruise}	1.004 (99.5%)	1.005 (99.4%)	1.045 (95.6%)	1.012 (98.8%)
	$k_{cruise-CD}$	0.900 (88.9%)	0.924 (91.8%)	0.902 (89.2%)	0.924 (91.8%)
	k_{CD}	0.812 (76.9%)	0.865 (84.4%)	0.773 (70.7%)	0.855 (83.1%)

B. Speed Experiment

1) Effect of speed distribution on conflict count: The conflict count per number of instantaneous aircraft is presented in Figures 14, 15, 16 and 17. The figures show that the conflict count does not vary much between speed distributions. When the expected horizontal relative velocity was calculated for different speed distributions, the numerical values were all really similar for every distribution type, to this was predicted.

The reason why the results overlap for all speed conditions is because the average speed is the same in for all tested cases. This means that the conflict count models are insensitive to the shape of the speed distribution, and are only affected by the value the average speed in an airspace volume of interest.

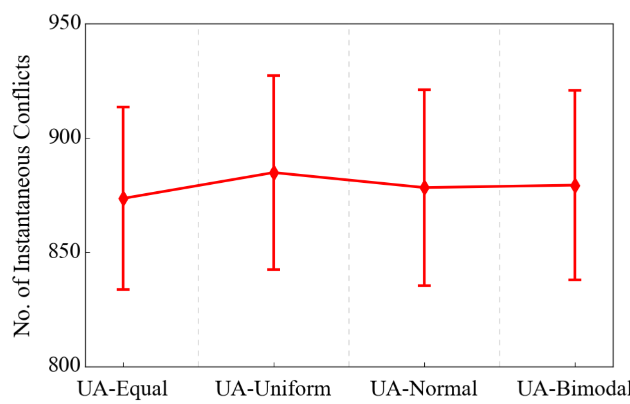

Figure 14. *Speed Experiment - The total number of instantaneous conflicts for the largest density being tested for Unstructured Airspace.*

2) Effect of speed distribution on model accuracy: Table IX shows the accuracies when the analytical model is fitted with the simulation results. The accuracies do not vary much from

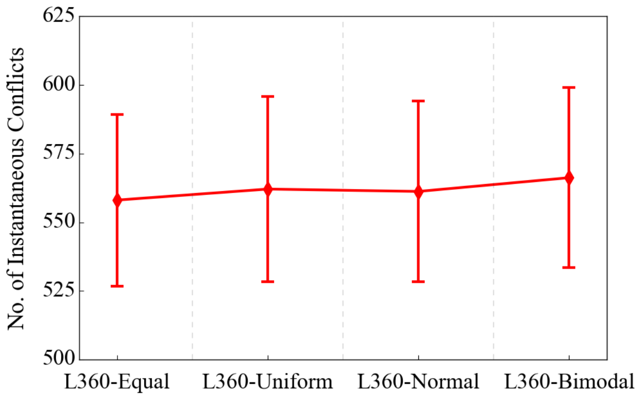

Figure 15. *Speed Experiment - The total number of instantaneous conflicts for the largest density being tested for the Layers 360 concept.*

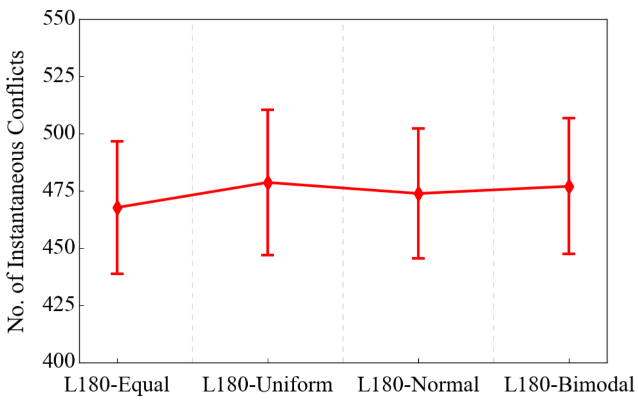

Figure 16. *Speed Experiment - The total number of instantaneous conflicts for the largest density being tested for the Layers 180 concept.*

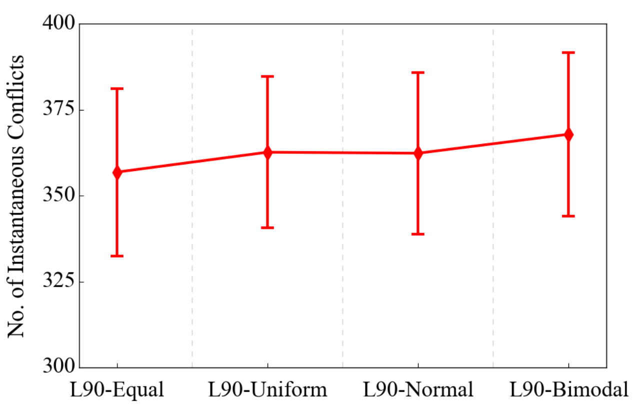

Figure 17. *Speed Experiment - The total number of instantaneous conflicts for the largest density being tested for the Layers 90 concept.*

the baseline scenario, which is where the speed distribution is equal.

The accuracies from the adjusted model is in Table XII. Using the numerically computed values still leads to good accuracies, they do not change much, but some get better and some get worse. This is mostly because of small changes in the expected horizontal relative velocity. Because $\bar{v}_{rel_h}$ does not change much, as can be seen in Table III, the accuracies were not expected to change much.

Table XI
SPEED: BASELINE k VALUES AND ACCURACY.

		Baseline Equal	Uniform	Normal	Bimodal
UA	k	1.024 (97.6%)	1.026 (97.4%)	1.026 (97.3%)	1.020 (97.9%)
L360	k_{cruise}	1.004 (99.5%)	0.997 (99.7%)	1.006 (99.3%)	1.003 (99.6%)
	$k_{cruise-CD}$	0.900 (88.9%)	0.898 (88.7%)	0.902 (89.2%)	0.907 (89.7%)
	k_{CD}	0.812 (76.9%)	0.850 (82.4%)	0.856 (83.2%)	0.860 (83.8%)
L180	k_{cruise}	0.995 (99.5%)	1.002 (99.7%)	1.005 (99.4%)	1.010 (98.9%)
	$k_{cruise-CD}$	0.897 (88.5%)	0.908 (89.9%)	0.901 (89.0%)	0.900 (88.9%)
	k_{CD}	0.814 (77.2%)	0.844 (81.6%)	0.829 (79.4%)	0.846 (81.8%)
L90	k_{cruise}	0.946 (94.3%)	0.960 (95.8%)	0.967 (96.6%)	0.974 (97.4%)
	$k_{cruise-CD}$	0.894 (88.1%)	0.891 (87.8%)	0.896 (88.4%)	0.896 (88.4%)
	k_{CD}	0.813 (77.1%)	0.837 (80.5%)	0.839 (80.8%)	0.855 (83.1%)

Table XII
SPEED: ADJUSTED k VALUES AND ACCURACY.

		Baseline Equal	Uniform	Normal	Bimodal
UA	k	1.024 (97.6%)	1.022 (97.7%)	1.029 (97.0%)	1.019 (98.0%)
L360	k_{cruise}	1.004 (99.5%)	0.992 (99.2%)	1.009 (99.0%)	1.001 (99.8%)
	$k_{cruise-CD}$	0.900 (88.9%)	0.895 (88.3%)	0.905 (89.5%)	0.906 (89.6%)
	k_{CD}	0.812 (76.9%)	0.846 (81.8%)	0.859 (83.6%)	0.859 (83.7%)
L180	k_{cruise}	0.995 (99.5%)	0.991 (99.1%)	1.007 (99.2%)	1.003 (99.6%)
	$k_{cruise-CD}$	0.897 (88.5%)	0.905 (89.5%)	0.904 (89.3%)	0.899 (88.8%)
	k_{CD}	0.814 (77.2%)	0.841 (81.1%)	0.832 (79.9%)	0.845 (81.7%)
L90	k_{cruise}	0.946 (94.3%)	0.928 (92.3%)	0.960 (95.8%)	0.949 (94.7%)
	$k_{cruise-CD}$	0.894 (88.1%)	0.888 (87.4%)	0.899 (88.7%)	0.895 (88.3%)
	k_{CD}	0.813 (77.1%)	0.833 (80.0%)	0.842 (81.2%)	0.854 (83.0%)

C. Altitude experiment

1) Effect of altitude distribution on conflict count: Figures 18 and 19 show that varying the altitude distribution changes the number of instantaneous conflict. It can be noted that a uniform altitude distribution causes the least number of conflicts. This suggests that the analytical model accuracy should be underestimating for the other altitude distributions.

2) Effect of altitude distribution on model accuracy: Table XIII shows the accuracies where the model was fitted with the data using the analytical model that is derived for a uniform altitude distribution scenario and the adjusted k values using

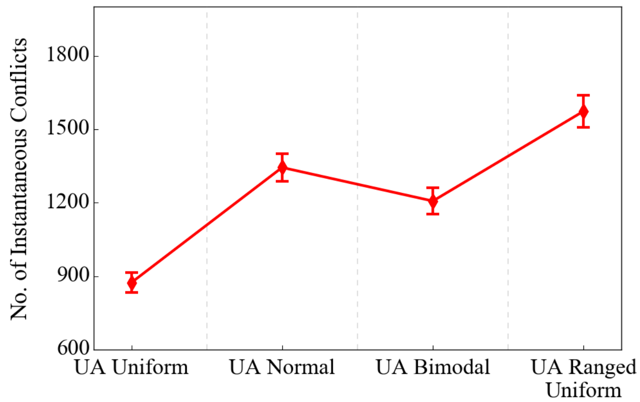

Figure 18. *Altitude Experiment - The total number of instantaneous conflicts for the largest density being tested for Unstructured Airspace.*

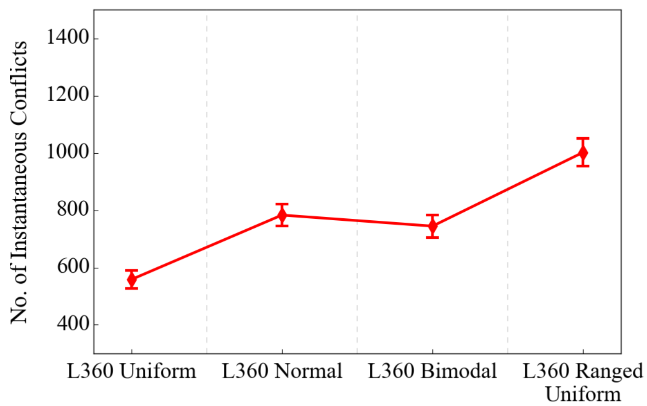

Figure 19. *Altitude Experiment - The total number of instantaneous conflicts for the largest density being tested for the Layers 360 concept.*

the numerical conflict count model. The baseline scenario has the uniform distribution. The accuracies were affected severely, the bimodal distribution was affected the least but very inaccurate still, but the other two distributions have very similar accuracies. For the layered concepts the ranged-uniform distribution had the worst accuracy. When the aircraft are distributed uniformly over half the altitude, it is expected that the conflicts will be twice as many. This was the results of the Layered concept experiments.

Table XIV shows the accuracy when the data is fitted with the adjusted model. When the values in Table IV for the UA, and Table V are the values used for the Layered concept. The accuracies are greatly improved when the adjustments are applied. In the Layered concept the $k_{cruise-C/D}$ and $k_{C/D}$ parameters are not changed, that is because the altitude distribution only affects the cruising aircraft. The accuracies work well for all scenarios, and the analytical model is applicable with the numerical adjustments.

D. Spatial Experiment

1) Effects of spatial distribution on conflict count: Figures 20, 21, 22 and 23 show the conflict count for the largest number of instantaneous aircraft for the baseline scenario and a scenario with a density hotspot. The conflict count is increased very significantly when the density is larger in one area.

Table XIII
ALTITUDE: BASELINE k VALUES AND ACCURACY.

		Baseline Uniform	Normal	Bimodal	Ranged Uniform
UA	k	1.024 (97.6%)	1.569 (63.7%)	1.416 (70.6%)	1.576 (63.4%)
L360	k_{cruise}	1.004 (99.5%)	1.664 (60.0%)	1.573 (63.5%)	2.041 (48.9%)
	$k_{cruise-CD}$	0.900 (88.9%)	0.936 (93.2%)	0.911 (90.3%)	0.914 (90.6%)
	k_{CD}	0.812 (76.9%)	0.870 (85.1%)	0.827 (79.1%)	0.766 (69.5%)

Table XIV
ALTITUDE: ADJUSTED k VALUES AND ACCURACY.

		Baseline Uniform	Normal	Bimodal	Ranged Uniform
UA	k	1.024 (97.6%)	1.102 (90.6%)	0.994 (99.4%)	0.957 (95.5%)
L360	k_{cruise}	1.004 (99.5%)	0.881 (86.6%)	0.894 (88.2%)	1.015 (98.4%)
	$k_{cruise-CD}$	0.900 (88.9%)	0.936 (93.2%)	0.911 (90.3%)	0.914 (90.6%)
	k_{CD}	0.812 (76.9%)	0.870 (85.1%)	0.827 (79.1%)	0.766 (69.5%)

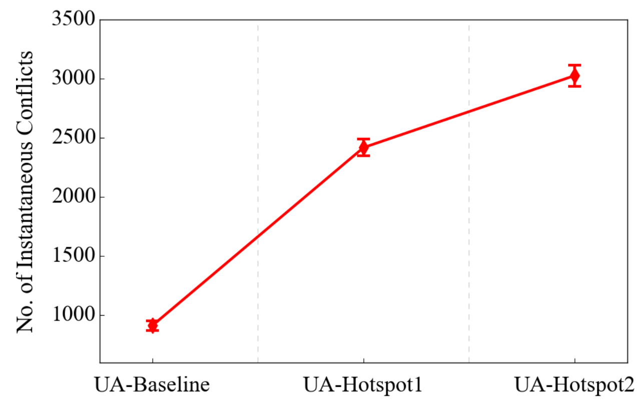

Figure 20. *Spatial Experiment - The total number of instantaneous conflicts for the largest density being tested for Unstructured Airspace.*

2) Effects of spatial distribution on model accuracy: In Table XV are the values when the simulation data is fitted with the baseline conflict count model. In general the accuracies are very low for the hotspot scenarios, except for aircraft that are climbing/descending. Table XVI shows the accuracy values when the conflict count form the simulations are fitted with the adjusted model. The accuracies are improved in all cases, and are even more accurate than the baseline model. This means that the model can be applied to different areas when dealing with a hotspot.

VI. DISCUSSION

This paper investigated the effect of traffic scenario related assumptions on the accuracy of analytical conflict count models for unstructured and layered airspace designs. Additionally,

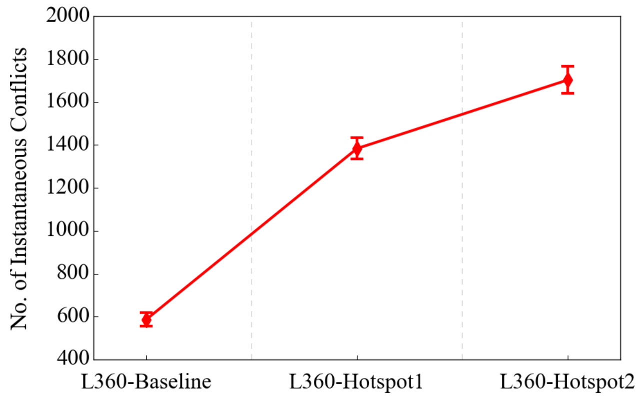

Figure 21. *Spatial Experiment - The total number of instantaneous conflicts for the largest density being tested for the Layers 360 concept.*

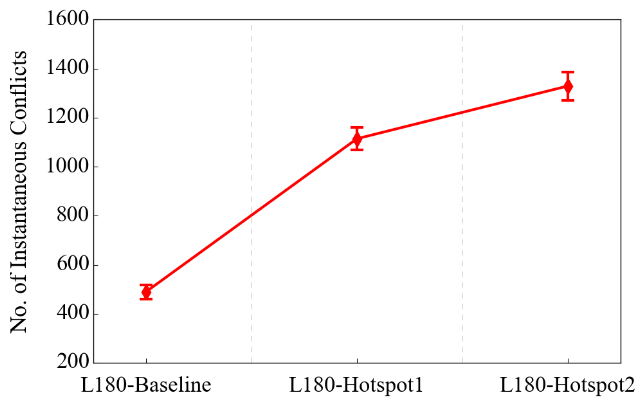

Figure 22. *Spatial Experiment - The total number of instantaneous conflicts for the largest density being tested for the Layers 180 concept.*

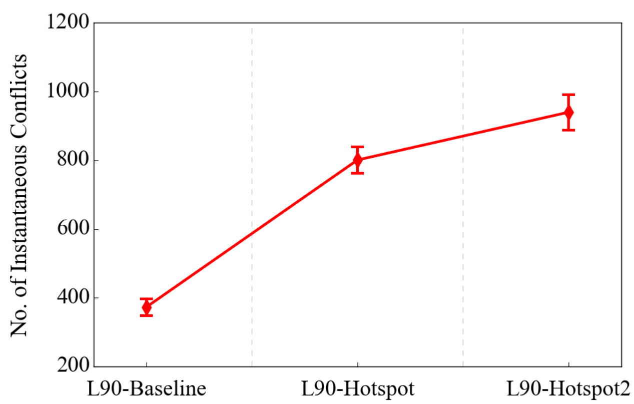

Figure 23. *Spatial Experiment - The total number of instantaneous conflicts for the largest density being tested for the Layers 90 concept.*

numerical methods were proposed as a means to improve model accuracies when traffic scenario assumptions are violated. The proposed methods were tested using 5 different fast-time simulation experiments. This section discusses the results of these experiments in relation to the main research questions of this study.

Table XV
SPATIAL: BASELINE k VALUES AND ACCURACY.

		Baseline Uniform	Hotspot 1	Hotspot 2
UA	k	1.025 (97.6%)	1.724 (57.9%)	2.077 (48.1%)
L360	k_{cruise}	1.004 (99.5%)	2.080 (48.0%)	2.575 (38.8%)
	$k_{cruise-CD}$	0.900 (88.9%)	0.561 (21.7%)	0.558 (20.8%)
	k_{CD}	0.812 (76.9%)	1.041 (96.0%)	1.114 (89.7%)
L180	k_{cruise}	0.995 (99.5%)	2.178 (45.9%)	2.616 (38.2%)
	$k_{cruise-CD}$	0.897 (88.5%)	0.563 (22.5%)	0.562 (22.2%)
	k_{CD}	0.814 (77.2%)	1.051 (95.0%)	1.121 (89.1%)
L90	k_{cruise}	0.946 (94.3%)	2.479 (40.3%)	2.972 (33.6%)
	$k_{cruise-CD}$	0.894 (88.1%)	0.585 (29.1%)	0.582 (28.3%)
	k_{CD}	0.813 (77.1%)	1.076 (92.8%)	1.141 (87.5%)

Table XVI
SPATIAL: ADJUSTED k VALUES AND ACCURACY.

		Baseline Uniform	Hotspot 1	Hotspot 2
UA	k	1.025 (97.6%)	0.906 (89.6%)	1.017 (98.2%)
L360	k_{cruise}	1.004 (99.5%)	1.035 (96.6%)	1.067 (93.6%)
	$k_{cruise-CD}$	0.900 (88.9%)	0.810 (88.7%)	0.824 (78.7%)
	k_{CD}	0.812 (76.9%)	0.752 (68.0%)	0.843 (81.5%)
L180	k_{cruise}	0.995 (99.5%)	1.083 (92.2%)	1.084 (92.2%)
	$k_{cruise-CD}$	0.897 (88.5%)	0.813 (77.1%)	0.829 (79.5%)
	k_{CD}	0.814 (77.2%)	1.049 (95.3%)	0.848 (82.2%)
L90	k_{cruise}	0.946 (94.3%)	1.232 (81.1%)	1.233 (81.0%)
	$k_{cruise-CD}$	0.894 (88.1%)	0.845 (81.6%)	0.851 (82.6%)
	k_{CD}	0.813 (77.1%)	1.073 (93.1%)	0.860 (83.8%)

A. Do the traffic scenario assumptions affect the accuracy of the analytical conflict count models?

Like mentioned before, the derivation of the model make certain assumptions. The heading distribution is assumed to be uniform. The speed is assumed to be equal for all aircraft. Aircraft are assumed to be spread evenly through all flight levels (uniform altitude distribution). The airspace that the model is being applied to, is assumed to have uniform density (uniform spatial distribution).

The heading distribution affects the expected horizontal relative velocity($\bar{v}_{rel_h}$). The analytical mode uses the baseline value for $\bar{v}_{rel_h}$ for all scenarios. The accuracy is affected the least when using bimodal heading distribution because the angle between two aircraft is more likely to be larger for a bimodal heading distribution than for a normal or ranged-uniform distributions expected relative velocity. The $\bar{v}_{rel_h}$

value is much lower for the normal distribution, and for the ranged-uniform. Those values are close to each other which is reflected in the results of the experiment. The normal distribution gives slightly better results than the ranged-uniform, but that is because $\bar{v}_{rel_h}$ is slightly greater.

The speed is another factor in computing the expected horizontal relative velocity. The results of the simulations do not show that the shape of the speed distribution has any significant effect on the expected horizontal relative velocity, as long as the average speed is the same. The results from non of the distribution that were being tested, stood out as different from the other. As the values for $\bar{v}_{rel_h}$ were all very similar, the speed distribution was not expected to affect the accuracies much, which proved to be the case.

The altitude distribution affects the unstructured and layered airspace differently. For the UA model, the uniform altitude distribution allows the conflict probability (p_2) to be expressed in terms of ratio between volume searched by the CD and the total volume of the airspace. But when the altitude distribution is not uniform the vertical part of the volume needs to be compensated for. The ranged-uniform altitude distribution was expected to have 50% accuracy because only half of the airspace is being used, but the actual accuracy is a bit higher. This is because the altitude distribution in the simulations affects mostly cruising aircraft. In the simulations the aircraft are being generated at a fixed time interval and all aircraft have the same climb rate, so climbing/descending aircraft still have a mostly uniform altitude distribution. The normal-, and bimodal distributions, were expected to have very close accuracies, because they have very similar p_v values (see Table V). Still the simulation results show that they differ some.

However the altitude distribution for layered concept affects the number of possible combinations of two aircraft. Because the height of each layer is larger than the vertical separation criteria, there is no chance of overlapping with an aircraft flying in a different altitude. The conflict count of each layer is computed as if it was a small airspace with only a single available flight level. The results for cruising-climbing/descending conflicts and climbing/descending conflicts were similarly accurate as the baseline scenario. The accuracies for the cruising conflicts were however much smaller. For the ranged-uniform distribution here, we can see that the accuracy is about half as accurate as the fully uniform distribution. Like stated earlier, only half of the altitudes are being used, so it is logical that there will be twice as many conflicts.

For the spatial distribution experiment, the accuracy was effected very much. The number conflicts were much higher than the baseline model suggested for UA and cruising aircraft in the layered concepts. Since all the cruising aircraft have to pass through the hotspot, the conflict probability is much higher for those aircraft. However, regarding conflict between cruising and climbing/descending aircraft, the model was over-estimating, but conflicts for only climbing/descending aircraft were actually more accurate than for the baseline scenario.

To summarize, the heading distribution does affect the accuracy of the analytical conflict count model. The varying speed does not seem to have much affect on the accuracy. The results for the altitude distributions show that when the aircraft are not spread evenly across all the altitudes, it has a significant affect on the accuracy. The spatial distribution has very large effect on the accuracy.

B. Which assumption has the largest effect on the accuracy?

Of the scenarios tested in this thesis, the hotspot in spatial distribution experiment causes the largest inaccuracies. When the altitude distribution is assumed to be uniform, it has much larger effect on the accuracy than the heading distribution, considering the traffic scenarios used in this research. While the speed distribution does not affect the model accuracy that much, it has the smallest effect.

C. Can numerical adjustments improve the accuracy of the models when the assumptions are violated?

In short, yes, the accuracies are improved by using the numerical values.

For the heading distribution, the adjustment that was applied showed very a good accuracy when the adjusted model was fitted with results from the experiments. When the numerically computed expected horizontal relative velocities (from Table II) are used to adjust the model, the accuracy for the normal-, and ranged-uniform distribution are improved greatly. But for the bimodal distribution the accuracy is decreases slightly. This might be because the simulations are stochastic and the difference in the accuracies is not very large. As stated earlier the accuracy for the bimodal distribution was already quite good so changes to the model did not affect the accuracy severely. In general, the conflict count model's flexibility is improved by using this adjustment.

Although the results from the speed experiments were quite accurate, the numerically computed values for the $\bar{v}_{rel_h}$ from Table III were used for adjustment. This improved some of the accuracies on a very small scale, while decreasing the accuracies of others. This change is minimal, and because the numerical values for $\bar{v}_{rel_h}$ were so close to the value used for the analytical model, this was expected. In the case of the speed assumption, an adjustment is not necessary but is still an option.

The values in Table IV are used to improve the inaccuracies for a non-uniform altitude distribution in unstructured airspace. The values are used as a part of the ratio between the volume searched by the CD and the total volume (as described in Section III). For normal and bimodal distributions, the values are the same. This is because the bimodal distribution is a distribution with two normal curves with half the size of the 'regular' normal distribution. When the values are derived the curves are integrated and it makes sense that they would yield the same value.

When the number of combinations is calculated for every layer instead of assuming the same number of aircraft in each layer. When the adjustment was applied, it resulted in improved accuracies for cruising aircraft. The other k parameters for layered airspace were unaffected, because the adjustment is not applied there.

The method to improve the accuracy for different spatial distributions is not really based on using numerically computed values like the other methods, but by applying the baseline model differently it may be improved. This method improves the accuracies for the scenario used in this paper. However, the application may have to be adjusted to the scenario that is being used. For example the airspace may have to be split up in more than two parts, which increases the number of terms in the equation.

D. Additional Considerations

The numerical methods presented in this paper to cope with traffic scenario assumptions have been tested for each assumption individually. In reality, it is likely that multiple aspects of traffic scenarios vary simultaneously; for example, both heading and altitude distributions are non-uniform for oceanic traffic. For such cases, the numerical adjustments for each individual traffic property can be combined, as long as the distribution shapes are known.

Some improvements can be made on the spatial distribution adjustment, by including the probability density function. This should be approached in a similar way as the altitude distribution adjustment is made, but for latitudinal and longitudinal distribution.

Although this research aims to investigate assumptions made in previous studies, there are still some assumptions made here. It is assumed that there is no effect from weather or terrain, and perfect aircraft state information is used for conflict detection. Although, climbing and descending aircraft are included, the scope of this research is limited to en-route airspace operations.

VII. CONCLUSION

The goal of this research was to study the effect of traffic scenario properties on the accuracy of analytical conflict count models for unstructured and layered airspace designs. The conflict count models have been derived assuming uniform heading and altitude distribution, an equal speed and the same density throughout the experiment area. Five experiments were performed: Four which addresses these assumptions and one which meets the assumptions, which is then used for comparison. Numerical adjustments to the models were made to compensate for the error caused by deviating by the ideal traffic scenario for the model. Then the accuracies of the analytical models without the adjustments were determined as well as the accuracies of the adjusted models. The following conclusions can be drawn:

- The analytical conflict count models are able to predict the shape of the relationship between the number of instantaneous conflicts and the instantaneous number of aircraft for all traffic scenario properties, but the accuracy decreases as the scenario assumptions are broken.
- The heading distribution affects the accuracy significantly.
- If all aircraft are assumed to have the same speed, it does not affect the accuracy significantly.
- Assuming a uniform altitude distribution causes large inaccuracies when the traffic scenario does not have a uniform altitude distribution.
- The accuracy for a traffic scenario with uneven traffic density can be improved by applying the analytical model to different specific sections of the airspace.
- The spatial distribution has a largest effect on the accuracy of the analytical model.
- The accuracy can be improved by augmenting the analytical models with numerically computed values of the number of combinations of aircraft, or the conflict probability between two aircraft, depending on the scenario assumption that is violated.

REFERENCES

[1] "Eurocontrol annual report," 2015.

[2] J. M. Hoekstra, R. C. J. Ruigrok, and R. Van Gent, "Free flight in a crowded airspace?" *Progress in Astronautics and Aeronautics*, vol. 193, pp. 533–546, 2001.

[3] M. Tra, "The effect of a layered airspace concept on conflict probability and capacity," 2016, MSc Thesis.

[4] E. Sunil, J. Ellerbroek, and J. M. Hoekstra, "Analysis of airspace structure and capacity for decentralized separation using fast-time simulations," *Journal of Guidance, Control and Dynamics*, vol. 40, pp. 38–51, 2017.

[5] M. R. Jardin, "Analytical relationships between conflict counts and air-traffic density," *Journal of Guidance, Control and Dynamics*, vol. 28, pp. 1150–1156, 2005.

[6] J. M. Hoekstra, J. Maas, M. Tra, and E. Sunil, "How do layered airspace design parameters affect airspace capacity and safety?" in *ICRAT confrence*, 2016.

[7] E. Sunil, J. Ellerbroek, J. Hoekstra, and J. Maas, "Three-dimensional conflict count models for unstructured and layered airpsace designs," Delft University of Technology.

[8] S. Endoh, "Aircraft collision models," MIT Department of Aeronautics and Astraonautics, Tech. Rep., 1982.

[9] J. M. Hoekstra and J. Ellerbroek, "Bluesky atc simulator project: an open data and open source approach," in *Research Gate*, 2016.